Spatial distribution of cloud droplet size properties from Airborne Hyper-Angular Rainbow Polarimeter (AirHARP) measurements

Brent A. McBride(1,2,3)*, J. Vanderlei Martins(1,2,3), Henrique M. J. Barbosa(4), William Birmingham(2,3), and Lorraine Remer(2,3)

(1)Department of Physics, University of Maryland Baltimore County, Maryland, USA
(2)Joint Center for Earth Systems Technology, Maryland, USA
(3)Earth and Space Institute, UMBC, Maryland, USA
(4)Instituto de Física, Universidade de São Paulo, São Paulo, Brasil

*Correspondence to Brent A. McBride at mcbride1@umbc.edu

Work adapted from McBride et al. (2019): "Spatial distributions of cloud droplet size properties from AirHARP measurements", Atmospheric Measurement Techniques Discussions. https://doi.org/10.5194/amt-2019-380

Background and Motivation

The liquid water cloud droplet size distribution (DSD) connects the microphysical and radiative impacts of clouds on climate, and therefore, is an important cloud property to measure with global coverage from space. Cloud droplet size is closely connected to way the droplet scatters light and the width of the distribution may be linked to cloud development and the onset of precipitation. Traditional radiometric measurements are information-limited in measuring the DSD: they can only access the droplet size, with no sensitivity to the distribution width, and are strongly affected by 3D shadowing and illumination effects. Polarimeter instruments can measure DSDs in an independent way: they access the entire DSD by sampling a single-scattering *cloudbow* structure that occurs at cloud top. Polarimeters can both improve and extend these traditional radiometric retrievals with wide swaths, high spatial and angular resolution, multi-spectral coverage, and high polarimetric accuracy.

The Hyper-Angular Rainbow Polarimeter (HARP) is a multispectral, multi-angle wide field-of-view (FOV) imaging polarimeter developed with the capability for global atmospheric measurements of the microphysical properties of clouds and aerosols. The three members of the HARP family (below) sample Earth scenes with a 114° along-track FOV and 120 unique views on the same target: 60 at 670nm, and 20 at 440, 550, and 870nm.

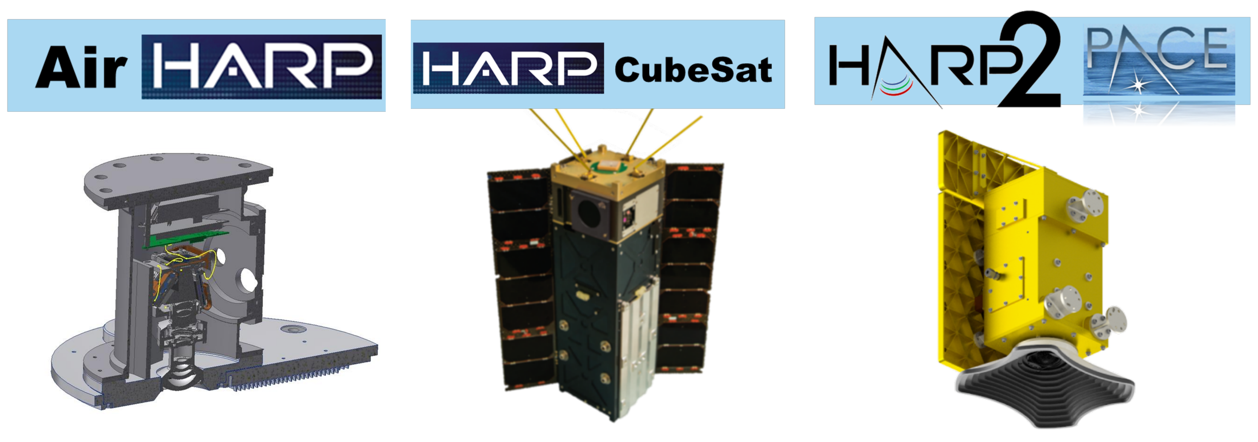

Airborne System	Launch – Nov. 2019	Launch - 2022-2023
• Ground calibration often • ~40m resolution • Deployed on NASA LMOS and ACEPOL campaigns	• Lower SNR • 4 km resolution • Limited data set: 1 snapshot/day	• Improved SNR • On-board calibration • ~3 km resolution • Global coverage in 2 days

Cloudbow Measurement from AirHARP

The AirHARP instrument can capture the full cloudbow structure in a single raw image (left), in this simulation from NASA LMOS. As the instrument flies, it takes data of the same cloud target at many viewing angles (middle). These views are aggregated into pushbrooms and all of them are co-located to a common grid (right).

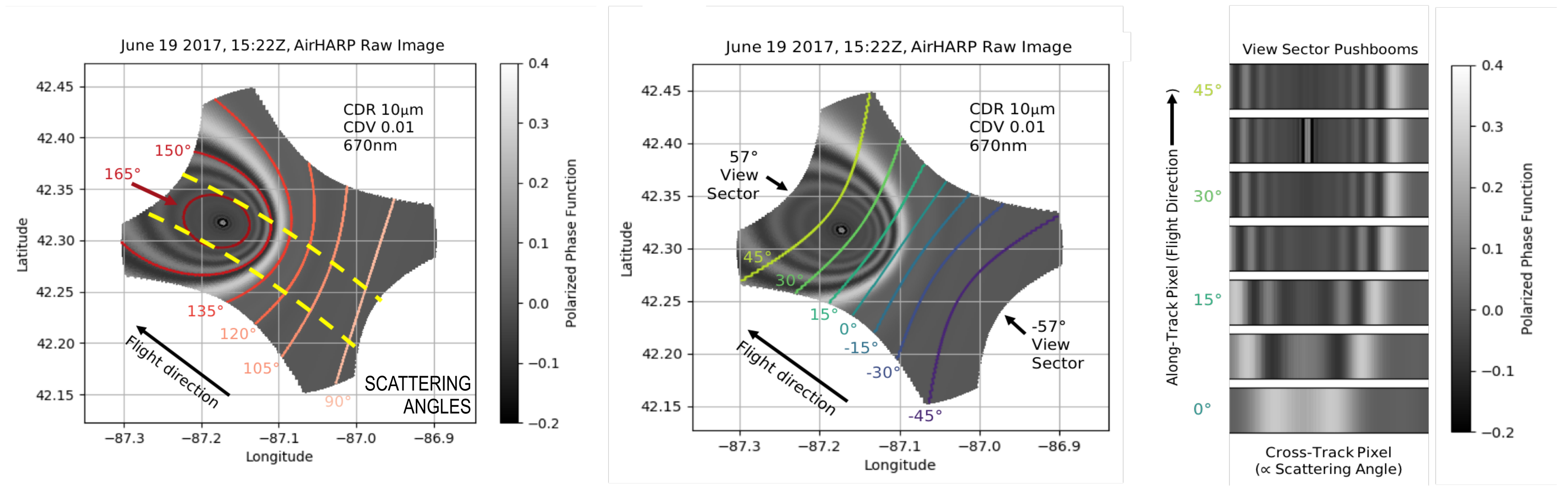

The scene from the same time and geometry as the above simulation. This is a RGB pushbroom composite of a stratocumulus cloud deck during NASA LMOS, observed near +30° view sector of the AirHARP detector. Each pixel is 50m.

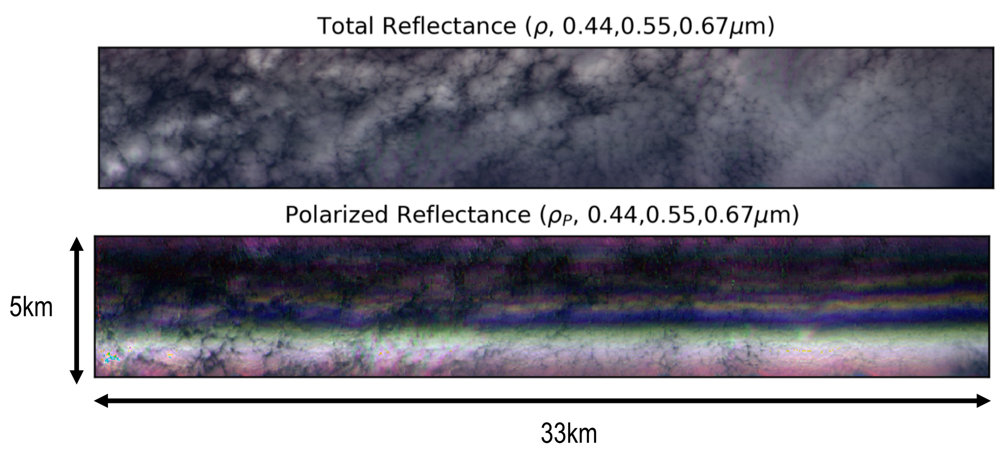

Using the co-registered pushbrooms, AirHARP can reconstruct the cloudbow at the pixel-level and yield a **spatial map of DSDs for any pixel with cloudbow geometry** (right).

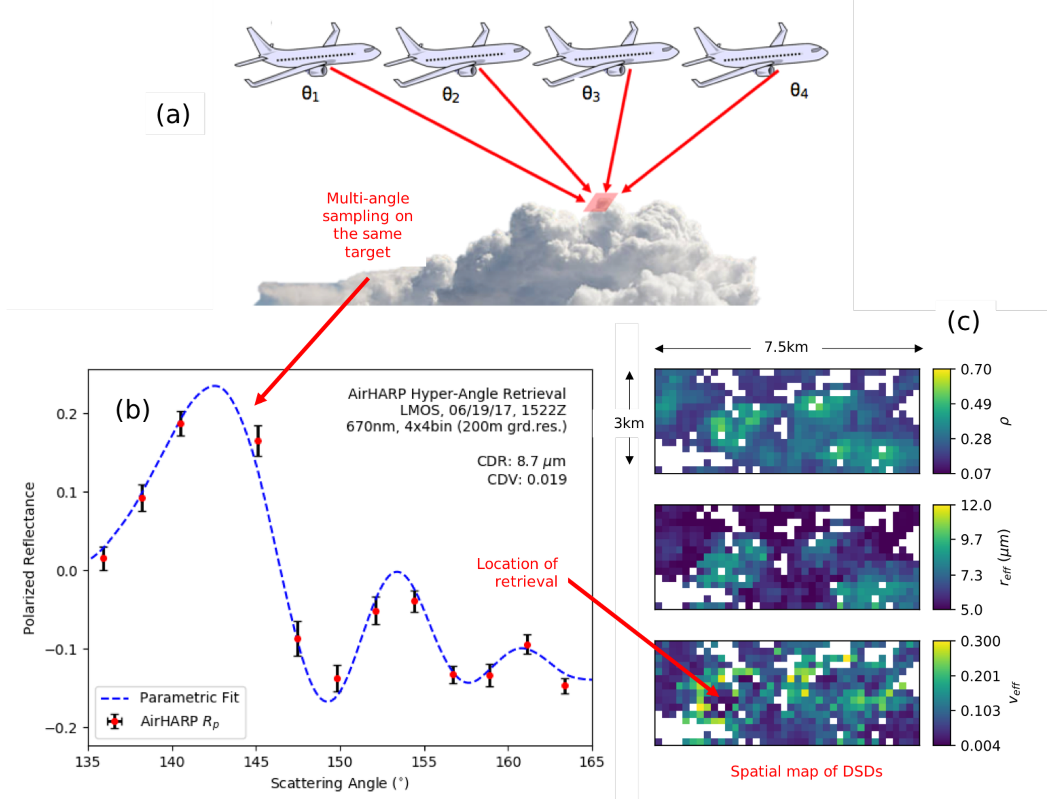

Polarization from Clouds

Liquid water clouds give off a highly directional structure at cloud top called the *polarized cloudbow (left).* The location of the cloudbow maxima with scattering angle is directly related to the area-weighted mean droplet size, the ***effective radius (CDR).*** The amplitude of the cloudbow maxima encodes the width of the size distribution, the ***effective variance (CDV)***.

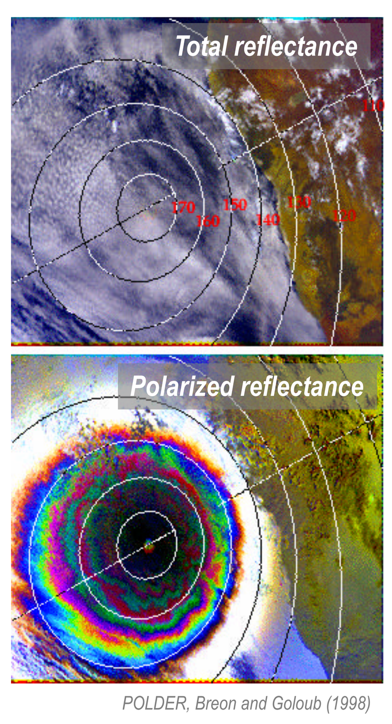

POLDER, Breon and Goloub (1998)

$$CDR = \frac{\int_0^\infty \pi r^3 n(r)\,dr}{\int_0^\infty \pi r^2 n(r)\,dr}$$

$$CDV = \frac{\int_0^\infty (r - CDR)^2 \pi r^2 n(r)\,dr}{CDR^2 \int_0^\infty \pi r^2 n(r)\,dr}$$

Hansen and Travis (1974)

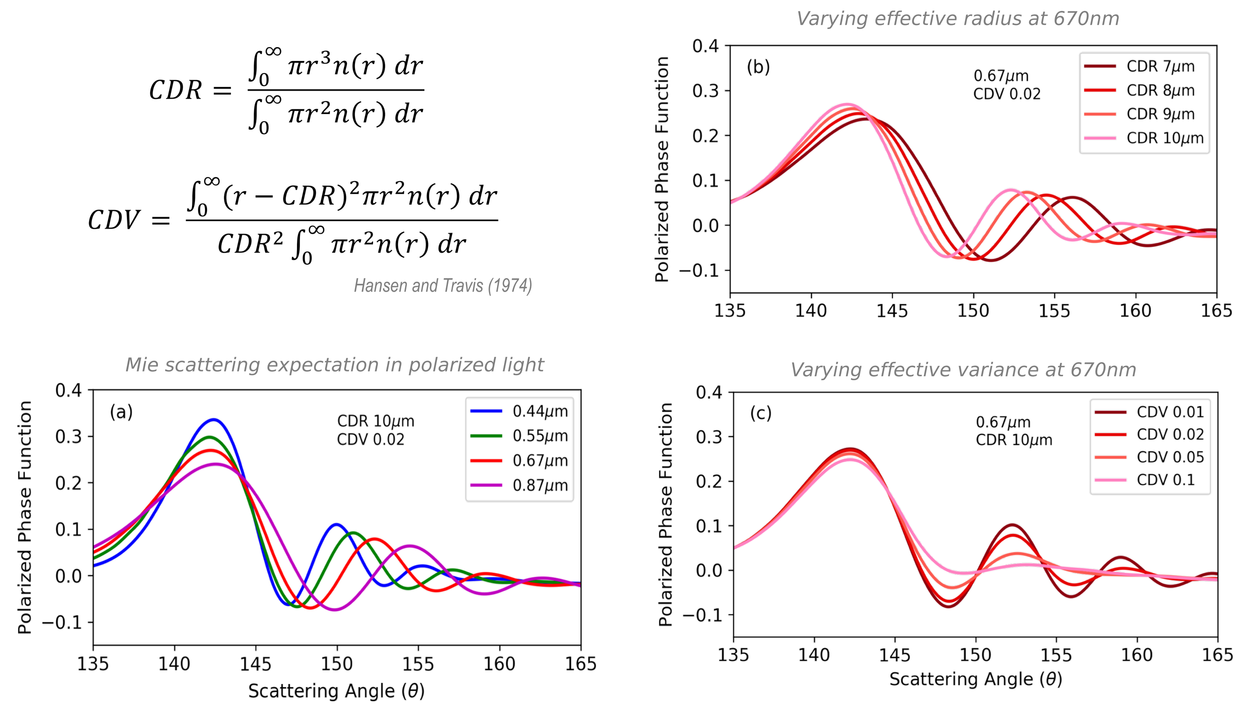

The polarized reflectance of the cloudbow is very similar to the expected polarized scattering of liquid water cloud droplets via Mie theory (the *polarized phase function)*. **Discrete measurements of the cloudbow structure can be compared directly to Mie curves using a look-up table approach to extract the CDR *and* CDV for a cloud target.** A modified gamma size distribution is assumed.

Polarimeter measurement

$$\mathcal{R}_{obs}(\lambda, \vartheta_{scat}) = \frac{4}{\pi}(\mu_0 + \mu)\left[\frac{-\pi Q_{sca}(\lambda, \vartheta_{scat})}{\mu_0 F_0}\right]$$

Mie simulation

$$\mathcal{R}_{fit}(\lambda, \vartheta_{scat}) = \alpha\langle P_{12}(\lambda, \vartheta_{scat}, CDR, CDV)\rangle + \beta \cos^2 \vartheta_{scat} + \gamma$$

Bulk scattering properties

$$\langle P_{12}(\lambda, \theta, CDR, CDV)\rangle = \frac{\sum_i P_{12,i}(\lambda, \theta, CDR, CDV)\omega_i(\lambda) C_{ext,i}(\lambda)}{\sum_i \omega_i(\lambda) C_{ext,i}(\lambda)}$$

This parametric fit technique also accounts for **non-cloud scatterers** with linear terms in scattering angle. This could be Rayleigh scattering, surface reflection, cirrus, aerosol, or geometric effects from rotating into the scattering plane.

In a sample cloudbow measurement from AirHARP (right), the polarized reflectance measurement is matched to the closest fitting Mie P12 and corrected for non-cloud scatterers.

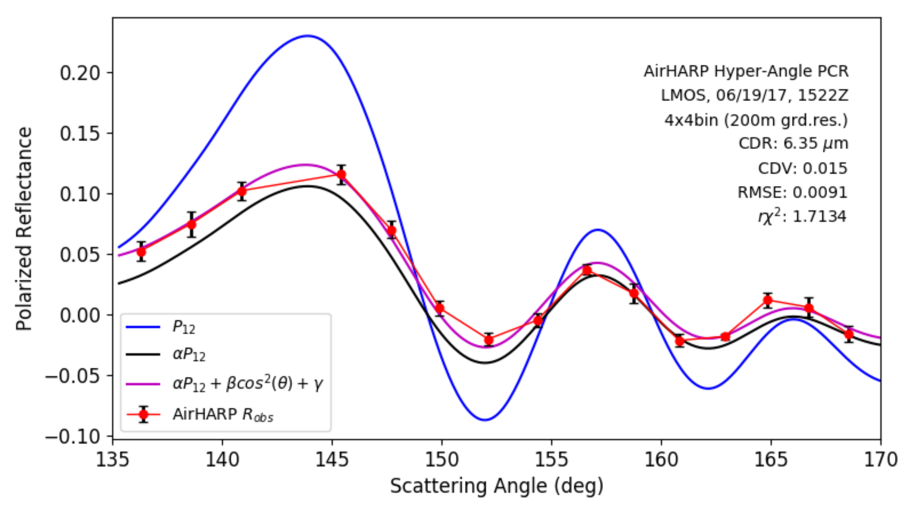

The best fitting Mie simulation is verified by thresholding the root-mean-square error and reduced chi-square of the parametric fit.

$$RMSE = \sqrt{\frac{1}{n}\sum_i^n \left(\mathcal{R}_{fit,i} - \mathcal{R}_{obs,i}\right)^2} \qquad \chi^2_{red} = \frac{1}{n-5}\sum_i^n \frac{\left(\mathcal{R}_{fit,i} - \mathcal{R}_{obs,i}\right)^2}{\sigma_{obs,i}^{\ 2}}$$

Comparison with LES

AirHARP cloud retrievals (above) compare well qualitatively with the ATEX clean case simulated by Miller et al. (2018). We see larger CDR and lower CDV in the cloud "cores" (defined by higher τ) and the opposite in cloud "periphery".

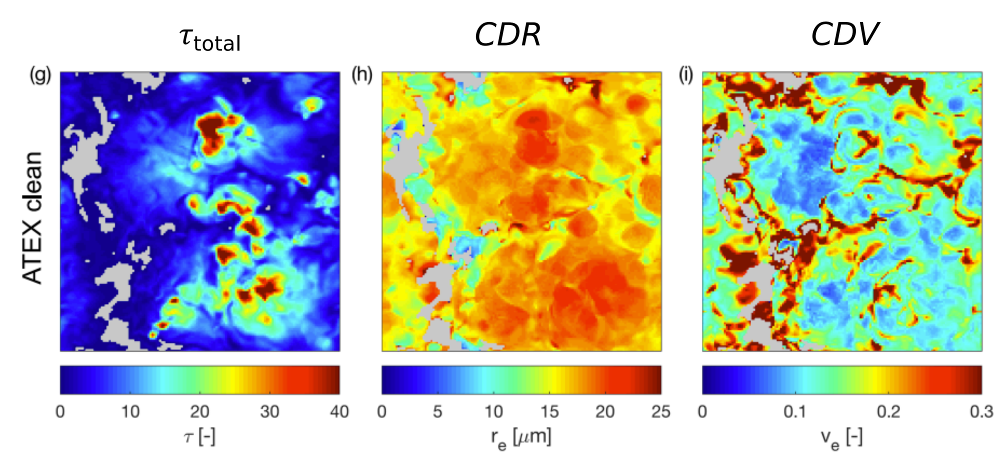

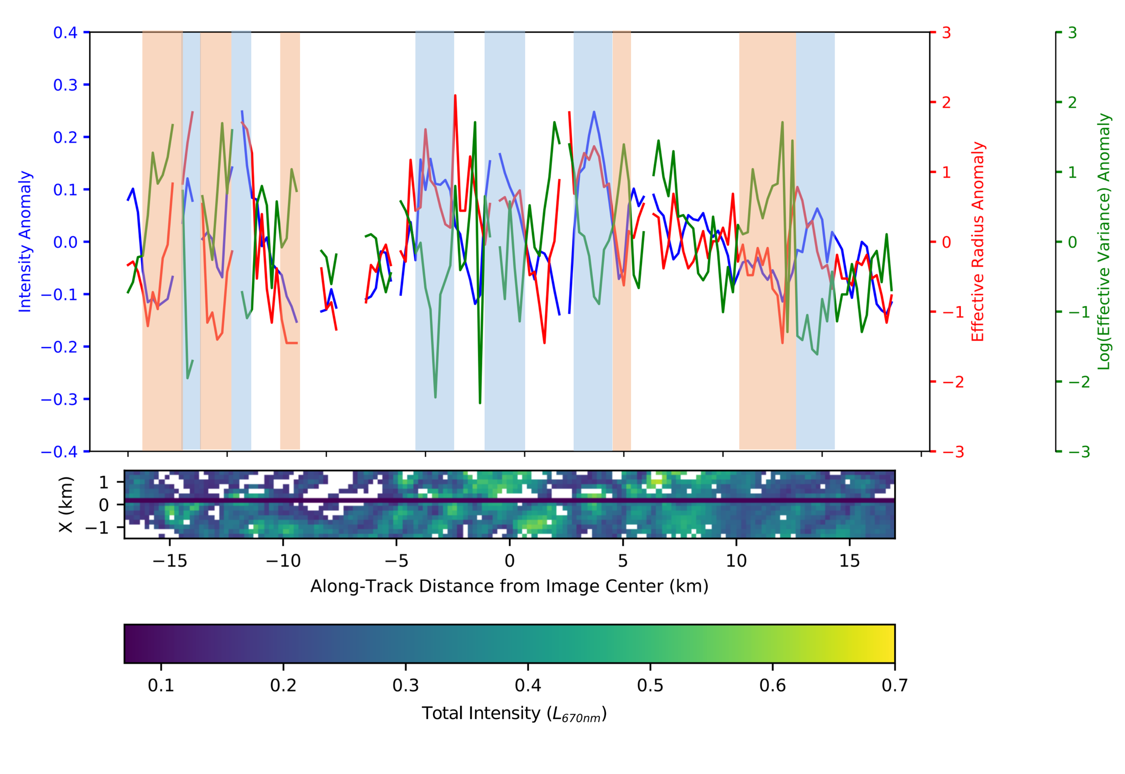

Phase Correlation of DSD Parameters

By taking a transect along the cloud field and normalizing each parameter by the transect mean, we can trend the parameters in cloud "core" (blue boxes) and "periphery" (orange boxes).

We find that the correlation between CDR and I is positive and negative with CDV in these areas. Each phase operates over 0.5-1km scales.

Effect of Resolution on Information Content

The polarized reflectance is aggregated and the retrieval is performed separately at 200m and 600m resolutions.

600m retrieval result is given above the boxes, while 200m results are reported in each sub-box. CDR in the middle column, CDV in last column. Retrieved P12 for 200m superpixels shown in gray for each case and 600m in red in the left plots.

We find the retrieval is robust for homogenous areas, but information content is lost at 600m when sub-pixel heterogeneity exists.

The larger retrieval resolution is similar to that of current MODIS and GOES-R ABI cloud droplet size retrieval products.

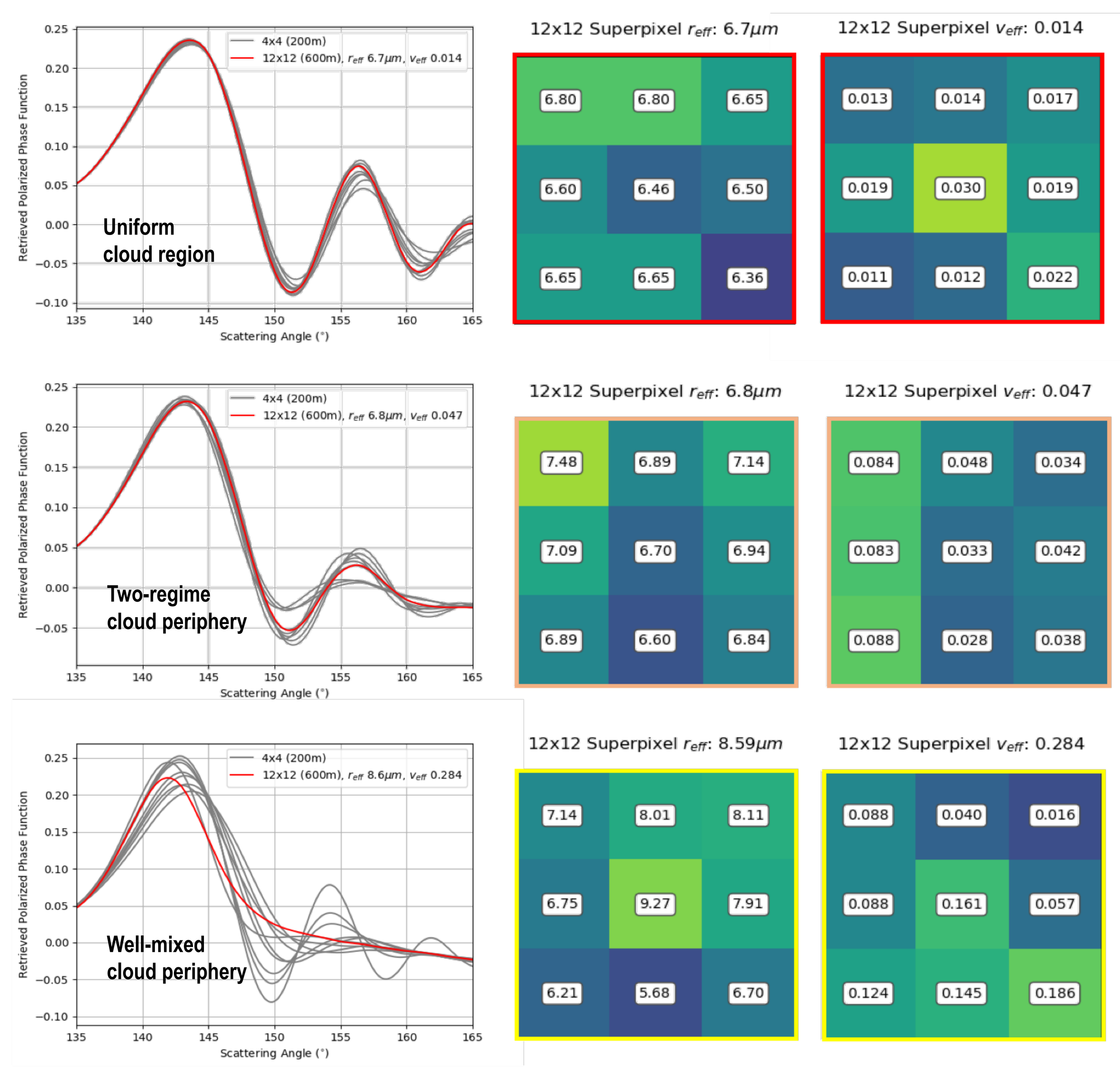

Acknowledgements

We acknowledge funding through the NASA Earth and Space Science Fellowship (NESSF) 16-EARTH16F-0243. Participation in APOLO made possible through U. of Iowa Travel Award.

UMBC